
Volume 37, January/February 2013
ELSEVIER
European Journal of
Mechanics
B/Fluids
Editors-in-Chief: F. Dias, Cachan (France) G.J.F. van Heijst, Eindhoven (Netherlands)
Associate Editors
P. Luchini, Salerno (Italy)
E.H. Meiburg, Santa Barbara (USA)
A. Thess, Ilmenau (Germany)
(Founded in 1961 as Journal de Mécanique)
www.elsevier.com/locate/ejmflu

European Journal of Mechanics B/Fluids 37 (2013) 187–194

Contents lists available at SciVerse ScienceDirect

European Journal of Mechanics B/Fluids

journal homepage: www.elsevier.com/locate/ejmflu

Reconstruction of the pressure in long-wave models with constant vorticity

Alfatih Ali, Henrik Kalisch *

Department of Mathematics, University of Bergen, Postbox 7800, 5020 Bergen, Norway

ARTICLE INFO

Article history:
Received 15 June 2012
Accepted 30 September 2012
Available online 9 October 2012

Keywords:
Surface waves
Long wave models
Pressure
Vorticity
Incompressible flow

ABSTRACT

The effect of constant background vorticity on the pressure beneath steady long gravity waves at the surface of a fluid is investigated. Using an asymptotic expansion for the streamfunction, we derive a model equation and a formula for the pressure in a flow with constant vorticity. The model equation was previously found by Benjamin (1962), [3], and is given in terms of the vorticity ω_0, and three parameters Q, R and S representing the volume flux, total head and momentum flux, respectively.

The focus of this work is on the reconstruction of the pressure from solutions of the model equation and the behavior of the surface wave profiles and the pressure distribution as the strength of the vorticity changes. In particular, it is shown that for strong enough vorticity, the maximum pressure is no longer located under the wave crest, and the fluid pressure near the surface can be below atmospheric pressure.

1. Introduction

It is well known that vorticity has a strong effect on the properties of surface waves in fluids. One important example is the propagation of waves over a shear current. In this case, it is convenient to consider the vorticity of the flow as a pre-existing condition, and to assume that the surface waves do not alter the background flow significantly [1]. In the linear case, this situation has been studied extensively. Indeed, the results of the linear theory are by now classical, and may be found in textbooks on the subject [2].

The present article focuses on the fluid pressure beneath a periodic train of surface waves in the nonlinear case. The starting point for our study is a long-wave equation for steady surface waves which was derived by Benjamin [3]. This equation is valid for steady nonlinear long gravity waves in the presence of constant background vorticity. As pointed out in [4], the case of constant vorticity is representative for the more general case of nonzero but non-constant vorticity, specifically in the case of waves whose wavelength is large when compared to the depth of the fluid.

As shown in [4], the features of finite-amplitude waves on a shear flow can be quite different from irrotational waves. In particular, the pressure below a wave crest may be below atmospheric pressure in the case of strong vorticity, and the maximum pressure may not be attained underneath the wavecrest. It is partially the purpose of the present article to demonstrate that such behaviour can already be captured at the level of simplified model equations in the case of long waves. In contrast, small amplitude surface waves in the presence of constant vorticity do not feature a non-monotone pressure function, as can be verified by examining the expression for the pressure derived in the linear approximation in [5].

The physical setup of the problem to be studied is given by a homogeneous fluid of undisturbed depth h_0 contained in a channel of unit width, and with an even bottom. The gravitational acceleration g acts in the negative z-direction, and there is a background shear flow with a linear velocity distribution and constant vorticity $-\omega_0$. The influence of transverse effects is assumed to be weak, so that the problem can be investigated in the two-dimensional case. Since this study is aimed at long waves, capillarity is neglected. The geometry of this situation is indicated in Fig. 1.

Following Benjamin and Lighthill [6], we define the volume flux per unit span due to the wave motion by Q, the momentum flux per unit span and unit density corrected for pressure force by S and the energy density per unit span by R. Defining the total depth from the free surface to the rigid bottom by the function $\zeta(x)$, and aiming for the description of steady long waves, an approximate governing equation for ζ takes the form

$$\left(Q + \frac{\omega_0}{2}\zeta^2\right)^2 \zeta'^2 = -3\left(\frac{\omega_0^2}{12}\zeta^4 + g\zeta^3 - (2R - \omega_0 Q)\zeta^2 + 2S\zeta - Q^2\right). \qquad (1.1)$$

This equation is expected to be a fair model of surface waves in the case when the waves are periodic, and the wavelength is larger than the undisturbed depth of the fluid. A more general long-wave equation allowing for arbitrary vorticity distribution was found in [3], but we will present a different derivation which will enable

* Corresponding author.
E-mail addresses: alfatih.ali@math.uib.no (A. Ali), henrik.kalisch@math.uib.no (H. Kalisch).

0997-7546/$ – see front matter © 2012 Elsevier Masson SAS. All rights reserved.
doi:10.1016/j.euromechflu.2012.09.009

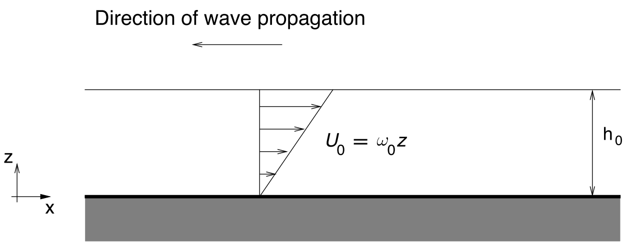

Fig. 1. This figure shows the background shear flow $U_0 = \omega_0 z$ when no wave motion is present. In the figure, ω_0 is positive, and an inertial reference frame is used. The waves which are superposed onto this background current propagate to the left.

us to obtain an approximate expression for the fluid pressure below the wave. As will be shown, the derivation of (1.1) is based on writing the streamfunction as an asymptotic expansion in terms of derivatives of $f(x)$, which represents the horizontal velocity at the bottom of the channel. The non-dimensional form of the expansion is given in terms of the small parameter $\beta = h_0^2/L^2$, where L is the wavelength. The Eq. (1.1) is found by disregarding terms of second and higher order in β in the integral expression for S.

Since (1.1) is a fully nonlinear equation, it is difficult to find solutions in closed form. However, a numerical scheme can easily be developed which yields approximate solutions of high accuracy. As is the custom in the study of incompressible fluids, the pressure is found from Bernoulli's equation. Since the problem is studied in two dimensions, the pressure can be expressed in terms of the streamfunction which in turn is given as an asymptotic expansion in the derivatives of f. Therefore, to find an approximation for the pressure for a given solution of (1.1), one needs to express f in terms of ζ. To this end, one may use the identity

$$Q = \frac{1}{2}\zeta^2\omega_0 + \zeta f - \zeta^3\frac{1}{6}f''$$

which will be shown to be valid to second order in β in Section 3.

To obtain an expression for f in terms of ζ, one has to invert the operator $1 - \frac{1}{6}\zeta^2\partial_{xx}$, leading to

$$\left[1 - \frac{1}{6}\zeta^2\partial_{xx}\right]^{-1}\left(\frac{Q}{\zeta} - \frac{1}{2}\zeta\omega_0\right) = f. \tag{1.2}$$

This identity, which is also valid to second order in β, will be used later in order to find the pressure as a function of ζ.

Before the main development is presented, it should be mentioned that there has been rapid recent progress in the mathematical understanding of wave properties with vorticity in the full water-wave problem for the Euler equations, such as the work presented in [7–14]. These studies focus on mathematical proofs of bifurcation, uniqueness and symmetry of periodic surface waves in the presence of vorticity. There are also a number of workers who have developed and used numerical schemes for the steady two-dimensional Euler equations with vorticity. Indeed, the studies presented in [15–19] mostly focus on constructing numerical approximations of surface wave profiles.

The authors of [20–22] have focused on the derivation of various time-dependent model equations for surface waves with vorticity, which are similar in spirit to Eq. (1.1). However, no discussion of the pressure was provided in these works. A mathematical proof of several qualitative properties of the pressure beneath a periodic irrotational surface wave was provided in [23]. The present study is related to the work in [24] where the dynamic pressure associated to time-dependent irrotational surface waves in the Boussinesq scaling was found asymptotically. The effect of vorticity on the modulational stability of periodic surface waves was investigated in [25]. In the presence of vorticity, even the linear problem still provides challenges, as testified to by the recent study [5] on particle paths in rotational linear surface waves, and the article [26] which focuses on the linear dispersion relation for surface waves in the context of non-constant vorticity.

The plan of the paper is as follows. In Section 2, the free-surface problem is formulated in terms of the Euler equations. In Section 3, a derivation of Eq. (1.1) is given, and in Section 4 it is shown how the pressure can be approximated. In Section 5, numerical computations are presented which clearly show the effect of vorticity on the shape of periodic traveling waves and the pressure distribution.

2. Formulation of the problem

Consider an incompressible and inviscid fluid of undisturbed depth h_0 running in a narrow open channel. If transverse effects can be neglected, the free-surface problem can then be studied in the (x, z)-plane, and the governing equations are the Euler equations, the continuity equation, and the usual bottom and free-surface boundary conditions [2]. If the focus is on steady periodic waves propagating to the left at a speed $c > 0$, it is convenient to use a traveling reference frame moving to the left at the same speed as the surface wave.

In the moving reference frame, the Euler equations are given by

$$\begin{aligned} UU_x + WU_z &= -\frac{P_x}{\rho}, \quad \text{in } 0 < z < \zeta(x), \\ UW_x + WW_z &= -\frac{P_z}{\rho} - g, \quad \text{in } 0 < z < \zeta(x), \end{aligned} \tag{2.1}$$

where P denotes the pressure, ζ is the total depth, and U and W are the horizontal and vertical velocities, respectively. The continuity equation is

$$U_x + W_z = 0, \quad \text{in } 0 < z < \zeta(x, t). \tag{2.2}$$

The bottom boundary condition is given by

$$W = 0, \quad \text{on } z = 0.$$

The surface boundary conditions are

$$\begin{aligned} &U\zeta' - W = 0, \quad \text{on } z = \zeta(x), \\ &P = 0, \quad \text{on } z = \zeta(x). \end{aligned}$$

For convenience, the pressure in the fluid is normalised to be zero when equal to atmospheric pressure. The continuity equation (2.2) guarantees the existence of the streamfunction ψ which satisfies the relations $U = \psi_z$, and $W = -\psi_x$. The vorticity is defined by $\omega = W_x - U_z$, and if constant vorticity $\omega = -\omega_0$ is stipulated, the above relations imply that

$$\Delta\psi = \psi_{xx} + \psi_{zz} = \omega_0, \quad \text{in } 0 < z < \zeta(x). \tag{2.3}$$

The kinematic boundary conditions are expressed in terms of the streamfunction ψ by

$$\psi_x = 0, \quad \text{on } z = 0, \tag{2.4}$$

$$\psi_z\zeta' + \psi_x = 0, \quad \text{on } z = \zeta(x). \tag{2.5}$$

The Euler equations (2.1) now take the form

$$\begin{aligned} \psi_z\psi_{xz} - \psi_x\psi_{zz} &= -P_x/\rho \quad \text{in } 0 < z < \zeta(x). \\ -\psi_z\psi_{xx} + \psi_x\psi_{xz} &= -P_z/\rho - g, \quad \text{in } 0 < z < \zeta(x). \end{aligned} \tag{2.6}$$

Integrating the system (2.6) and making use of (2.3) shows that the quantity

$$\frac{1}{2}\psi_z^2 + \frac{1}{2}\psi_x^2 - \omega_0\psi + P/\rho + gz \tag{2.7}$$

must be constant throughout the fluid domain. Since the streamfunction is constant on the free surface, and in light of the dynamic boundary condition $P = 0$ on the free surface, we have the condition

$$\frac{1}{2}\psi_z^2 + \frac{1}{2}\psi_x^2 + g\zeta = R, \quad \text{on } z = \zeta(x). \tag{2.8}$$

The constant R represents the energy per unit mass per unit span [6], and the quantity R/g is usually called total head. Finally, combining (2.7) and (2.8) shows that the pressure can be expressed as

$$P = \rho\left(R - gz - \frac{1}{2}(\psi_x^2 + \psi_z^2) + \omega_0\psi - \omega_0 Q\right), \tag{2.9}$$

where Q is the value of the streamfunction ψ at the free surface. If we stipulate that ψ be equal to zero at the streamline along the flat bottom, then Q denotes the total volume flux per unit width given by

$$Q = \int_0^{\zeta} \psi_z dz. \tag{2.10}$$

Taking the derivative of (2.10) and using the kinematic boundary conditions (2.4) and (2.5) we get $\frac{dQ}{dx} = 0$, which shows the volume flux across a cross-section in the flow is independent of the location x. Now, the momentum flux per unit width and unit density S may be defined by

$$\begin{aligned} S &= \int_0^{\zeta}\left\{\frac{P}{\rho} + \psi_z^2\right\} dz \\ &= \int_0^{\zeta}\left\{R - gz - \frac{1}{2}\psi_x^2 + \frac{1}{2}\psi_z^2 + \omega_0\psi - \omega_0 Q\right\} dz. \end{aligned} \tag{2.11}$$

The derivation of the Eq. (1.1) is based on the fact that S is constant as a function of x. In order to show this fact, the above expression is differentiated with respect to x. The derivative is

$$\begin{aligned} \frac{dS}{dx} &= \int_0^{\zeta} \{-\psi_x\psi_{xx} + \psi_z\psi_{xz} + \omega_0\psi_x\}\, dz \\ &\quad + \zeta'\left[R - gz - \frac{1}{2}\psi_x^2 + \frac{1}{2}\psi_z^2 - \omega_0 Q + \omega_0\psi\right]_{z=\zeta}. \end{aligned}$$

Using Eq. (2.3) and the bottom boundary condition (2.4), we find that

$$\begin{aligned} \frac{dS}{dx} &= -\psi_z^2\zeta'|_{z=\zeta} \\ &\quad + \zeta'\left[R - gz - \frac{1}{2}\psi_x^2 + \frac{1}{2}\psi_z^2 - \omega_0 Q + \omega_0\psi\right]_{z=\zeta} \\ &= \zeta' R - \zeta'\left[gz + \frac{1}{2}\psi_x^2 + \frac{1}{2}\psi_z^2\right]_{z=\zeta} = 0. \end{aligned}$$

In the context of the irrotational problem, it has been shown that the three parameters Q, R and S determine a unique traveling wave profile. This was done first in the context of the KdV equation [6], then indicated numerically for the full Euler equations [27], and finally proved mathematically [28] for certain parameter values of R. The Q, R and S parameter space for the irrotational problem has been analyzed in [29].

3. Derivation of the model equation

For rotational flow with constant vorticity $-\omega_0$, the horizontal velocity is split into the two parts U_0 and U_1, where $U_0 = \omega_0 z$ is the background shear velocity, and U_1 is the horizontal component of the velocity due to the wave motion (see Fig. 2). We assume that the perturbation (U_1, W_1) of the velocity field is irrotational, so that the streamfunction can be written as $\psi = \frac{1}{2}z^2\omega_0 + \psi_1$, where ψ_1 satisfies Laplace's equation. Next, we use the standard expansion of the stream function in powers of the vertical variable z

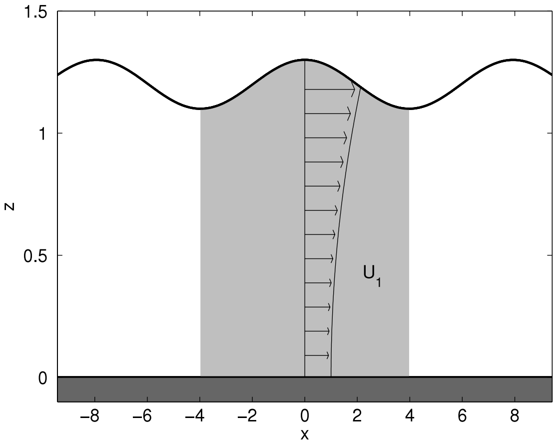

Fig. 2. This figure indicates the fundamental domain on which the streamfunction ψ is to be found. The bottom is shaded dark grey, and the periodic domain is shaded light grey. The variables are non-dimensional. In the traveling reference frame moving to the left at the speed c, the wave is stationary, and the horizontal fluid velocity U_1 is directed towards the right.

$$\psi = \frac{1}{2}z^2\omega_0 + \sum_{m=1}^{\infty} z^m f_m(x),$$

where $f_m(x)$ are unknown functions. The vorticity equation (2.3) and the boundary condition at the bottom (2.4) imply that

$$\psi = \frac{1}{2}z^2\omega_0 + \sum_{k=0}^{\infty}\frac{(-1)^k z^{(2k+1)}}{(2k+1)!}\frac{\partial^{2k} f}{\partial x^{2k}},$$

for $f = f_1$ which represents the horizontal velocity at the bottom. In order to express this problem in non-dimensional variables, we use the scaling

$$\tilde{x} = \frac{x}{L}, \qquad \tilde{z} = \frac{z}{h_0}, \qquad \tilde{\zeta} = \frac{\zeta}{h_0},$$

$$\tilde{\psi} = \frac{1}{c_0 h_0}\psi, \qquad \tilde{\omega}_0 = \frac{h_0}{c_0}\omega_0,$$

where $c_0 = \sqrt{gh_0}$ represents the limiting long-wave speed, and L is the wavelength of the periodic wave. In addition, the quantities Q, S and R are scaled by

$$\tilde{Q} = \frac{Q}{h_0 c_0}, \qquad \tilde{S} = \frac{S}{h_0 c_0^2}, \qquad \tilde{R} = \frac{R}{c_0^2}.$$

The non-dimensional expression for ψ appears as

$$\tilde{\psi} = \frac{1}{2}\tilde{z}^2\tilde{\omega}_0 + \tilde{z}\tilde{f} - \frac{\beta}{3!}\tilde{z}^3\tilde{f}'' + \frac{\beta^2}{5!}\tilde{z}^5\tilde{f}^{(4)} + \mathcal{O}(\beta^3). \tag{3.1}$$

The function $\tilde{f}$ can be approximated using the condition that $\tilde{\psi} = \tilde{Q}$ at the free surface, which yields

$$\tilde{f} = \frac{\tilde{Q}}{\tilde{\zeta}} - \frac{1}{2}\tilde{\zeta}\tilde{\omega}_0 + \frac{\beta}{6}\tilde{\zeta}^2\tilde{f}'' + \mathcal{O}(\beta^2). \tag{3.2}$$

The non-dimensional momentum flux is given by

$$\tilde{S} = \int_0^{\tilde{\zeta}}\left\{\tilde{R} - \tilde{z} - \frac{1}{2}\beta\tilde{\psi}_{\tilde{x}}^2 + \frac{1}{2}\tilde{\psi}_{\tilde{z}}^2 + \tilde{\omega}_0\tilde{\psi} - \tilde{\omega}_0\tilde{Q}\right\} d\tilde{z}, \tag{3.3}$$

Substituting for $\tilde{\psi}$ the expression found in (3.1) we obtain

$$\begin{aligned} \tilde{S} = \int_0^{\tilde{\zeta}} \Bigg\{ & \tilde{R} - \tilde{z} - \frac{1}{2}\beta\left(\tilde{z}^2\tilde{f}'^2 + \mathcal{O}(\beta)\right) \\ & + \frac{1}{2}\left(\tilde{z}^2\tilde{\omega}_0^2 + 2\tilde{z}\tilde{\omega}_0\tilde{f} + \tilde{f}^2 - \beta\tilde{\omega}_0\tilde{z}^3\tilde{f}'' - \beta\tilde{z}^2\tilde{f}\tilde{f}'' + \mathcal{O}(\beta^2)\right) \\ & + \tilde{\omega}_0\left(\frac{1}{2}\tilde{z}^2\tilde{\omega}_0 + \tilde{z}\tilde{f} - \frac{\beta}{6}\tilde{z}^3\tilde{f}'' + \mathcal{O}(\beta^2)\right) - \tilde{\omega}_0\tilde{Q}\Bigg\}\, d\tilde{z}. \end{aligned}$$

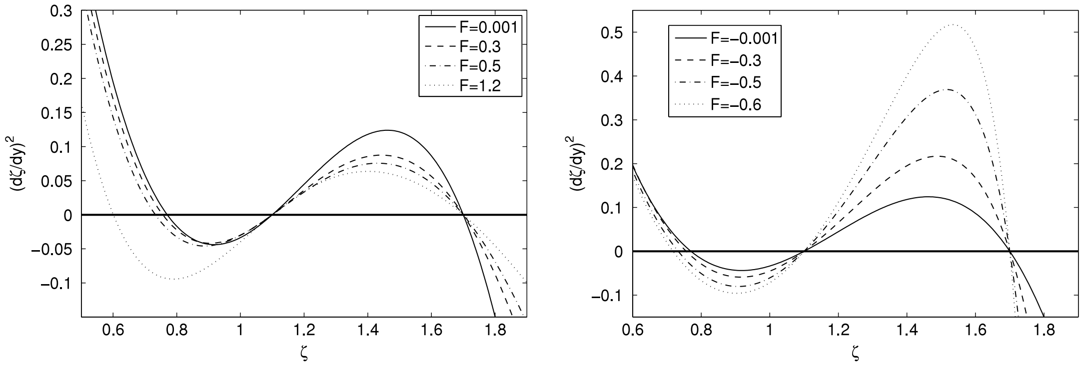

(a) $\omega_0 > 0$. (b) $\omega_0 < 0$.

Fig. 3. Plot of ζ'^2 as a function of ζ with different values of F. Note that the solutions oscillate between the minimum m and the maximum M which are the same for all curves.

Integrating with respect to $\tilde{z}$ yields

$$\tilde{S} = \tilde{R}\tilde{\zeta} - \frac{1}{2}\tilde{\zeta}^2 - \frac{\beta}{6}\tilde{\zeta}^3\tilde{f}'^2 + \frac{1}{2}\tilde{\zeta}\tilde{f}^2 - \frac{\beta}{6}\tilde{\zeta}^3\tilde{f}\tilde{f}'' + \frac{1}{3}\tilde{\zeta}^3\tilde{\omega}_0^2 + \tilde{\omega}_0\tilde{\zeta}^2\tilde{f} - \frac{\beta}{6}\tilde{\omega}_0\tilde{\zeta}^4\tilde{f}'' - \tilde{\omega}_0\tilde{Q}\tilde{\zeta} + \mathcal{O}(\beta^2).$$

Substituting for $\tilde{f}$ the expression found in (3.2), the non-dimensional momentum flux is therefore obtained in the form

$$\begin{aligned}\tilde{S} = {} & \tilde{R}\tilde{\zeta} - \frac{1}{2}\tilde{\zeta}^2 - \frac{\beta}{6}\tilde{\zeta}^3\left[\tilde{Q}^2\frac{\tilde{\zeta}'^2}{\tilde{\zeta}^4} + \tilde{\omega}_0\tilde{Q}\frac{\tilde{\zeta}'^2}{\tilde{\zeta}^2} + \frac{1}{4}\tilde{\omega}_0^2\tilde{\zeta}'^2\right] \\ & + \frac{1}{2}\tilde{\zeta}\left[\frac{\tilde{Q}^2}{\tilde{\zeta}^2} - \tilde{Q}\tilde{\omega}_0 + \frac{1}{4}\tilde{\zeta}^2\tilde{\omega}_0^2 + \frac{\beta}{3}\tilde{Q}\tilde{\zeta}\tilde{f}'' - \frac{\beta}{6}\tilde{\omega}_0\tilde{\zeta}^3\tilde{f}''\right] \\ & - \frac{\beta}{6}\tilde{\zeta}^3\left[\frac{\tilde{Q}}{\tilde{\zeta}}\tilde{f}'' - \frac{1}{2}\tilde{\omega}_0\tilde{\zeta}\tilde{f}''\right] + \frac{1}{3}\tilde{\zeta}^3\tilde{\omega}_0^2 - \tilde{\omega}_0\tilde{Q}\tilde{\zeta} \\ & + \tilde{\omega}_0\tilde{\zeta}^2\left[\frac{\tilde{Q}}{\tilde{\zeta}} - \frac{1}{2}\tilde{\zeta}\tilde{\omega}_0 + \frac{\beta}{6}\tilde{\zeta}^2\tilde{f}''\right] - \frac{\beta}{6}\tilde{\omega}_0\tilde{\zeta}^4\tilde{f}'' + \mathcal{O}(\beta^2).\end{aligned}$$

Now as intimated in the Introduction, the second derivative of $\tilde{f}$ may be expressed in terms of $\tilde{\zeta}$ and its derivatives in the form

$$\tilde{f}'' = 2\tilde{Q}\frac{\tilde{\zeta}'^2}{\tilde{\zeta}^3} - \tilde{Q}\frac{\tilde{\zeta}''}{\tilde{\zeta}^2} - \frac{1}{2}\tilde{\omega}_0\tilde{\zeta}'' + \mathcal{O}(\beta). \tag{3.4}$$

Indeed, this formula follows from differentiating (1.2) twice, and dropping terms of order β. Using this substitution, and disregarding terms of second order in β, the expression for $\tilde{S}$ reduces to

$$\begin{aligned}\tilde{S} = {} & \tilde{R}\tilde{\zeta} - \frac{1}{2}\tilde{\zeta}^2 - \frac{\beta}{6}\tilde{Q}^2\frac{\tilde{\zeta}'^2}{\tilde{\zeta}} + \frac{1}{2}\frac{\tilde{Q}^2}{\tilde{\zeta}} \\ & - \frac{1}{2}\tilde{Q}\tilde{\omega}_0\tilde{\zeta} - \frac{1}{24}\tilde{\omega}_0^2\tilde{\zeta}^3 - \frac{\beta}{6}\tilde{Q}\tilde{\omega}_0\tilde{\zeta}\tilde{\zeta}'^2 - \frac{\beta}{24}\tilde{\omega}_0^2\tilde{\zeta}^3\tilde{\zeta}'^2.\end{aligned} \tag{3.5}$$

Multiplying Eq. (3.5) by $2\tilde{\zeta}$ and rearranging yields

$$\begin{aligned}& \frac{\beta}{3}\left(\tilde{Q} + \frac{\tilde{\omega}_0}{2}\tilde{\zeta}^2\right)^2\tilde{\zeta}'^2 \\ & = -\left(\frac{\tilde{\omega}_0^2}{12}\tilde{\zeta}^4 + \tilde{\zeta}^3 - (2\tilde{R} - \tilde{\omega}_0\tilde{Q})\tilde{\zeta}^2 + 2\tilde{S}\tilde{\zeta} - \tilde{Q}^2\right).\end{aligned} \tag{3.6}$$

In dimensional form, this equation is (1.1). Solving (1.1) for ζ'^2 yields

$$\zeta'^2 = \frac{-3\left(\frac{\omega_0^2}{12}\zeta^4 + g\zeta^3 - (2R - \omega_0 Q)\zeta^2 + 2S\zeta - Q^2\right)}{\left(Q + \frac{\omega_0}{2}\zeta^2\right)^2}. \tag{3.7}$$

In the case that $\omega_0 = 0$, Eq. (3.7) becomes

$$\varphi'^2 = -3\,\frac{g\varphi^3 - 2\hat{R}\varphi^2 + 2\hat{S}\varphi - \hat{Q}^2}{\hat{Q}^2}, \tag{3.8}$$

where $\hat{Q}$, $\hat{R}$, $\hat{S}$ are computed in the absence of the vorticity. The Eq. (3.8) is the steady KdV equation derived by Benjamin–Lighthill in [6]. Let φ_1, φ_2 and φ_3 denote the roots of the cubic polynomial in Eq. (3.8). If $\varphi_3 < \varphi_2 < \varphi_1$, then Eq. (3.8) has cnoidal wave solutions given by

$$\varphi(z) = \varphi_2 + (\varphi_1 - \varphi_2)\,\mathrm{cn}^2\left(\sqrt{\frac{3(\varphi_1 - \varphi_3)}{4(\hat{Q}^2/g)}}\,z;\ r\right). \tag{3.9}$$

where cn is the Jacobian elliptic function with the modulus $r = \frac{\varphi_1 - \varphi_2}{\varphi_1 - \varphi_3}$. The constants $\hat{Q}$, $\hat{R}$ and $\hat{S}$ are obtained in the form

$$\hat{Q} = (g\varphi_1\varphi_2\varphi_3)^{\frac{1}{2}},$$
$$\hat{R} = \frac{g}{2}(\varphi_1 + \varphi_2 + \varphi_3),$$
$$\hat{S} = \frac{g}{2}(\varphi_1\varphi_2 + \varphi_1\varphi_3 + \varphi_2\varphi_3).$$

In order to understand the transition of surface wave patterns on a quiescent background state to waves on a shear flow, it is expedient to compare the cubic polynomial in (3.8) to the rational function representing $(\zeta')^2$ from (3.7). Denoting by M the maximum value of a given solution of (3.7), it is convenient to measure the strength of the background vorticity against the mass flux due to the wave motion by defining the non-dimensional number F by

$$F = \frac{\omega_0 M^2}{2Q}.$$

In some works this number is referred to as the Froude number. Curves for several positive and negative values of F with Q, R and S fixed are shown in Fig. 3. Note that the curves for $F = 0$ and very small values of F are visually indistinguishable.

4. Approximating the pressure

Before we set out to solve (1.1), an approximate formula for the pressure corresponding to a surface profile ζ is found. Using the expression (2.9) and the scaling $\tilde{P} = \frac{P}{\rho c_0^2}$, the non-dimensional pressure is found in the form

$$\tilde{P} = \tilde{R} - \tilde{z} - \frac{1}{2}(\beta\tilde{\psi}_{\tilde{x}}^2 + \tilde{\psi}_{\tilde{z}}^2) + \tilde{\omega}_0\tilde{\psi} - \tilde{\omega}_0\tilde{Q}.$$

Therefore, using the ansatz for $\tilde{\psi}$, we obtain

$$\begin{aligned}\tilde{P} &= \tilde{R} - \tilde{z} - \frac{1}{2}\beta\tilde{z}^2\tilde{f}'^2 \\ &\quad - \frac{1}{2}\left(\tilde{z}^2\tilde{\omega}_0^2 + 2\tilde{z}\tilde{\omega}_0\tilde{f} + \tilde{f}^2 - \beta\tilde{\omega}_0\tilde{z}^3\tilde{f}'' - \beta\tilde{z}^2\tilde{f}\tilde{f}''\right) \\ &\quad - \tilde{\omega}_0\tilde{Q} + \tilde{\omega}_0\left(\frac{1}{2}\tilde{z}^2\tilde{\omega}_0 + \tilde{z}\tilde{f} - \frac{\beta}{6}\tilde{z}^3\tilde{f}''\right) + \mathcal{O}(\beta^2),\end{aligned}$$

which gives

$$\begin{aligned}\tilde{P} &= \tilde{R} - \tilde{z} - \frac{\beta}{2}\tilde{z}^2\tilde{f}'^2 - \frac{1}{2}\tilde{f}^2 + \frac{\beta}{2}\tilde{z}^2\tilde{f}\tilde{f}'' \\ &\quad + \frac{\beta}{3}\tilde{\omega}_0\tilde{z}^3\tilde{f}'' - \tilde{\omega}_0\tilde{Q} + \mathcal{O}(\beta^2).\end{aligned}$$

In similar way as for the momentum flux, using the substitution (3.2) for $\tilde{f}$ and a similar relation for $\tilde{f}'$ yields

$$\begin{aligned}\tilde{P} &= \tilde{R} - \tilde{z} - \frac{\beta}{2}\tilde{z}^2\left[\tilde{Q}^2\frac{\tilde{\zeta}'^2}{\tilde{\zeta}^4} + \tilde{\omega}_0\tilde{Q}\frac{\tilde{\zeta}'^2}{\tilde{\zeta}^2} + \frac{1}{4}\tilde{\omega}_0^2\tilde{\zeta}'^2\right] \\ &\quad - \frac{1}{2}\left[\frac{\tilde{Q}^2}{\tilde{\zeta}^2} - \tilde{Q}\tilde{\omega}_0 + \frac{1}{4}\tilde{\zeta}^2\tilde{\omega}_0^2 + \frac{\beta}{3}\tilde{Q}\tilde{\zeta}\tilde{f}'' - \frac{\beta}{6}\tilde{\omega}_0\tilde{\zeta}^3\tilde{f}''\right] \\ &\quad + \frac{\beta}{2}\tilde{z}^2\left[\frac{\tilde{Q}}{\tilde{\zeta}}\tilde{f}'' - \frac{1}{2}\tilde{\omega}_0\tilde{\zeta}\tilde{f}''\right] - \frac{\beta}{3}\tilde{\omega}_0\tilde{z}^3\tilde{f}'' - \tilde{\omega}_0\tilde{Q} + \mathcal{O}(\beta^2).\end{aligned}$$

Cancellations and further rearrangements lead to

$$\begin{aligned}\tilde{P} &= \tilde{R} - \tilde{z} - \frac{\beta}{2}\tilde{z}^2\tilde{\zeta}'^2\left[\frac{\tilde{Q}}{\tilde{\zeta}^2} + \frac{\tilde{\omega}_0}{2}\right]^2 - \frac{\tilde{\zeta}^2}{2}\left[\frac{\tilde{Q}}{\tilde{\zeta}^2} + \frac{\tilde{\omega}_0}{2}\right]^2 \\ &\quad + \frac{\beta}{2}\left[\frac{\tilde{\omega}_0}{6}\tilde{\zeta}^3 - \frac{\tilde{Q}}{3}\tilde{\zeta} + \tilde{z}^2\frac{\tilde{Q}}{\tilde{\zeta}} - \frac{\tilde{\omega}_0}{2}\tilde{z}^2\tilde{\zeta} - \frac{2}{3}\tilde{\omega}_0\tilde{z}^3\right]\tilde{f}'' + \mathcal{O}(\beta^2).\end{aligned}$$

Using the expression for $\tilde{f}''$ found in (3.4), we see that the pressure is given by

$$\begin{aligned}\tilde{P} &= \tilde{R} - \tilde{z} - \frac{\beta}{2}\left(\frac{\tilde{Q}}{\tilde{\zeta}^2} + \frac{\tilde{\omega}_0}{2}\right)^2(\tilde{z}^2\tilde{\zeta}'^2 + \tilde{\zeta}^2) \\ &\quad + \frac{1}{2}\left(\frac{\tilde{\omega}_0}{6}\tilde{\zeta}^3 - \frac{\tilde{Q}}{3}\tilde{\zeta} + \beta\tilde{z}^2\frac{\tilde{Q}}{\tilde{\zeta}} - \frac{\tilde{\omega}_0}{2}\tilde{z}^2\tilde{\zeta} - \frac{2}{3}\tilde{\omega}_0\tilde{z}^3\right) \\ &\quad \times\left(2\tilde{Q}\frac{\tilde{\zeta}'^2}{\tilde{\zeta}^3} - \tilde{Q}\frac{\tilde{\zeta}''}{\tilde{\zeta}^2} - \frac{1}{2}\tilde{\omega}_0\tilde{\zeta}''\right) + \mathcal{O}(\beta^2).\end{aligned}$$

By neglecting terms of second order in β and reverting to dimensional variables, the pressure formula becomes

$$\begin{aligned}P &= \rho\Bigg\{R - gz - \frac{1}{2}\left(\frac{Q}{\zeta^2} + \frac{\omega_0}{2}\right)^2(z^2\zeta'^2 + \zeta^2) \\ &\quad + \frac{1}{2}\left(\frac{\omega_0}{6}\zeta^3 - \frac{\omega_0}{2}z^2\zeta - \frac{2}{3}\omega_0 z^3 - \frac{Q}{3}\zeta + z^2\frac{Q}{\zeta}\right) \\ &\quad \times\left(2Q\frac{\zeta'^2}{\zeta^3} - \zeta''\left(\frac{Q}{\zeta^2} + \frac{1}{2}\omega_0\right)\right)\Bigg\}, \end{aligned} \tag{4.1}$$

which represents the pressure approximation up to second order in β. In the case where vorticity effects are neglected, i.e. when $\omega_0 = 0$, the corresponding expression reduces to

$$\begin{aligned}\hat{P} &= \rho\Bigg\{\hat{R} - gz - \frac{1}{2}\left(\frac{\hat{Q}}{\varphi^2}\right)^2(z^2\varphi'^2 + \varphi^2) \\ &\quad + \frac{1}{2}\left(z^2\frac{\hat{Q}}{\varphi} - \frac{\hat{Q}}{3}\varphi\right)\left(2\hat{Q}\frac{\varphi'^2}{\varphi^3} - \varphi''\frac{\hat{Q}}{\varphi^2}\right)\Bigg\}. \end{aligned} \tag{4.2}$$

5. Numerical results

In this section we study smooth solutions of Eq. (1.1) and take a look at the corresponding pressure distributions. Note first that the Eq. (3.7) can be written in the form

$$\zeta'^2 = \frac{\mathcal{G}(\zeta)}{\mathcal{F}(\zeta)}.$$

To study the transition from irrotational waves to waves on a background flow with constant vorticity, we keep the mass flux Q and the amplitude of the wave constant. Denoting the maximum of a wave profile by M and the minimum by m, we thus keep the parameters Q, M and m fixed. As noted in [6], the undisturbed depth is given by $h_0 = \sqrt[3]{gQ^2}$, so that the undisturbed depth is then also constant.

Then if Z_1, Z_2, m, and M represent the roots of the numerator $\mathcal{G}$ on the right-hand side of (3.7), one may write

$$\begin{aligned}\mathcal{G}(\zeta) &= -3\left(\frac{\omega_0^2}{12}\zeta^4 + g\zeta^3 - (2R - \omega_0 Q)\zeta^2 + 2S\zeta - Q^2\right) \\ &= \frac{\omega_0^2}{4}(M-\zeta)(\zeta-m)(\zeta-Z_1)(\zeta-Z_2). \end{aligned} \tag{5.1}$$

By comparing the coefficients in (5.1) and assuming that Q, m, and M are given, the two additional roots Z_1 and Z_2 can be found as

$$\begin{aligned}Z_1 &= \frac{1}{2}\Bigg(-\left(\frac{12}{\omega_0^2}g + (M+m)\right) \\ &\qquad - \sqrt{\left(\frac{12}{\omega_0^2}g + (M+m)\right)^2 + \frac{24Q^2}{\omega_0^2 mM}}\Bigg), \\ Z_2 &= \frac{1}{2}\Bigg(-\left(\frac{12}{\omega_0^2}g + (M+m)\right) \\ &\qquad + \sqrt{\left(\frac{12}{\omega_0^2}g + (M+m)\right)^2 + \frac{24Q^2}{\omega_0^2 mM}}\Bigg). \end{aligned} \tag{5.2}$$

Moreover, the total head R and the momentum flux S can be obtained by

$$\begin{aligned}R &= \frac{w_0 Q}{2} - \frac{\omega_0^2}{24}\left(Z_1Z_2 + mM + (M+m)(Z_1+Z_2)\right), \\ S &= -\frac{\omega_0^2}{24}\left((M+m)Z_1Z_2 + mM(Z_1+Z_2)\right). \end{aligned} \tag{5.3}$$

Depending on the sign of ω_0, there are two cases. If $\omega_0 > 0$, then ζ'^2 has no singularities, and the integration is straightforward. There is a smooth periodic solution if $Z_2 < m < M$, (note that (5.2) implies $Z_1 < Z_2$). This situation is shown in panel (a) of Fig. 3, where only Z_2, m and M are shown, as the first root Z_1 is very large in absolute value.

If $\omega_0 < 0$, then ζ'^2 has two singularities, and the parameter space will be more restricted. In order to find the singularities, we express $\mathcal{F}(\zeta)$ as

$$\mathcal{F}(\zeta) = \left(Q + \frac{\omega_0}{2}\zeta^2\right)^2 = \frac{\omega_0^2}{4}(\zeta - A_+)^2(\zeta - A_-)^2$$

which reveals that the derivative is singular when ζ takes the values $A_+ = \sqrt{\frac{2Q}{-\omega_0}}$ and $A_- = -\sqrt{\frac{2Q}{-\omega_0}}$.

In the case $\omega_0 < 0$, smooth solutions exist only with the condition $M < A_+$. The phase plane picture is indicated in panel (b) of Fig. 3. The singularities at $\zeta = A_+$ and $\zeta = A_-$ are not shown in Fig. 3, but it can be inferred that as $|F|$ increases, A_+ gets closer to M, and moves in from the right.

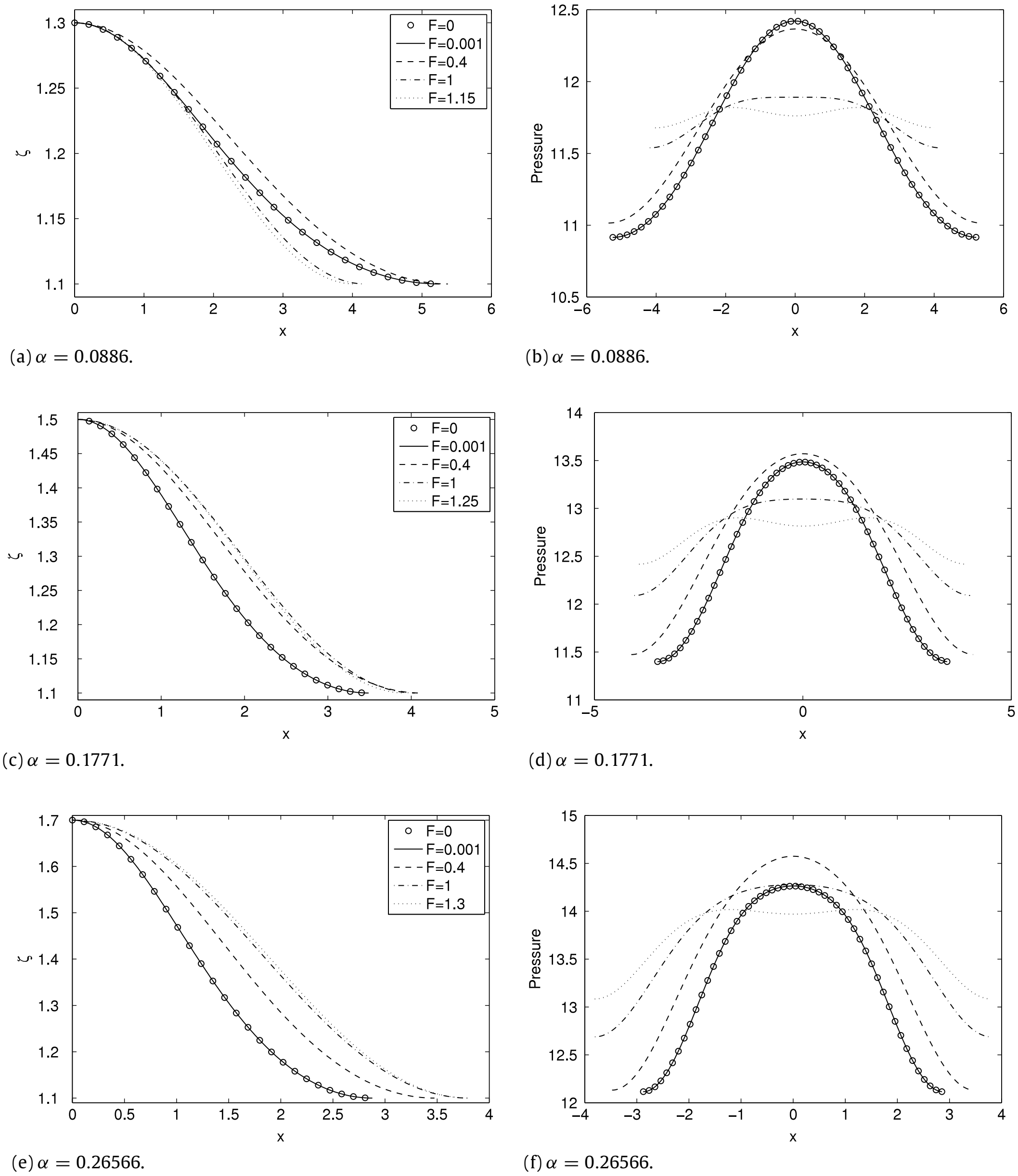

Fig. 4. For each case, from the top to the bottom, the amplitude α is fixed and the solution of (1.1) is found using different positive values of F. The left panels show one half wavelength of the wave profile and the right panels show the corresponding pressure evaluated at the channel bed. For the case $F = 0$, the exact cnoidal-wave solution (3.9) and the pressure expression (4.2) are used.

Having examined the parameter space of smooth solutions, a standard integration shows that solutions of (1.1) are given implicitly by

$$|x - x_0| = \int_{\zeta_0}^{\zeta} \frac{\left(\frac{2}{\omega_0}Q + \xi^2\right)}{\sqrt{(M-\xi)(\xi-m)(\xi-Z_1)(\xi-Z_2)}}\,d\xi. \qquad (5.4)$$

where $\zeta(x_0) = \zeta_0$, $M = \max_{x\in\mathbb{R}} \zeta(x)$ is the wave crest and $m = \min_{x\in\mathbb{R}} \zeta(x)$ represents the wave trough. Integrating from $\zeta_0 = m$ to the maximum wave height M gives half of the wavelength, however the integral (5.4) will have two singularities at the points $\zeta = m$ and $\zeta = M$. Fortunately, these singularities can be removed by using the transformation

$$\zeta = m + (M - m)\sin^2 t. \qquad (5.5)$$

Thus (5.4) is transformed into

$$|x - x_0| = 2\int_0^{\pi/2} \frac{\left(A + (2m\sin^2 t + (M-m)\sin^4 t)\right)}{\sqrt{(B+\sin^2 t)(C+\sin^2 t)}}\,dt, \qquad (5.6)$$

where

$$A = \frac{\frac{2}{w_0}Q + m^2}{M - m}, \qquad B = \frac{m - Z_2}{M - m}, \quad \text{and} \quad C = \frac{m - Z_1}{M - m}.$$

Now it is clear that this integral has no singularities since $B > 0$ and $C > 0$. The implicit solution is given as a grid function $x_j = x(\zeta_j) \in \left[x_0, \frac{L}{2}\right]$, where L represents the full wavelength. In order to obtain ζ as a function of x on a regular grid, a spline interpolation can be used, such as described for example in [30,31].

To investigate the effect of background vorticity on the waves and associated flows, we perform several numerical experiments to solve Eq. (1.1) while gradually increasing the parameter F. The numerical solutions are then substituted into (4.1) to find the corresponding pressure. Figs. 4 and 5 each display three sets of experiments with three different amplitudes. The nondimensional amplitude α used in these experiments is given by $\alpha = (M - m)/2h_0$. where h_0 is found from Q as mentioned before. When using very small vorticity $\omega_0 \approx 0$, the solutions of (1.1) are nearly

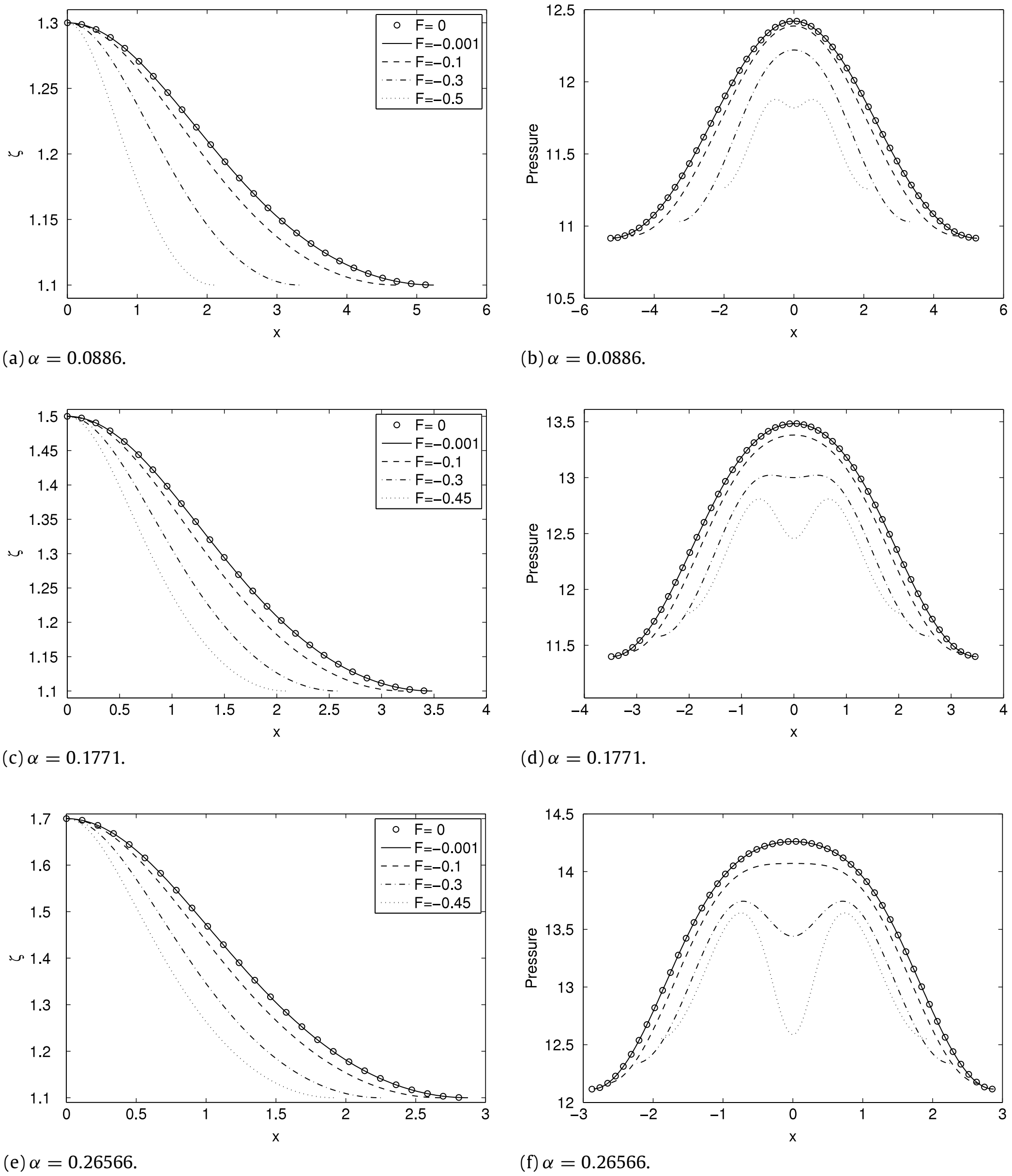

(a) $\alpha = 0.0886$. (b) $\alpha = 0.0886$.

(c) $\alpha = 0.1771$. (d) $\alpha = 0.1771$.

(e) $\alpha = 0.26566$. (f) $\alpha = 0.26566$.

Fig. 5. For each case, from the top to the bottom, the amplitude α is fixed and the solution of (1.1) is found using different negative values of F. The left panels show the wave profile and the right panels show the corresponding pressure at the channel bed. For the case $F = 0$, the exact cnoidal-wave solution (3.9) and the pressure expression (4.2) are used.

indistinguishable from the cnoidal-wave solutions of Eq. (3.8) (cf. Figs. 5(a) and 4(a)). As expected in this case, the pressure is also similar to the irrotational pressure (4.2). As shown in Figs. 4 and 5, stronger vorticity leads to more pronounced deviation in both the wave profile, and the total pressure profile at the bottom.

In the case of positive F, the wave profile first becomes wider, and then with increasing F, the profile becomes narrower again (this is not shown in panel (e) of Fig. 4 since very large values of F are needed to see this trend if the amplitude is not small). In all cases with positive F, increasing the vorticity beyond $F = 1$ causes a non-monotonicity in the pressure profile. Indeed, as the three panels on the right in Fig. 4 show, the maximum pressure at the bottom of the channel does not occur beneath the wave crest.

A further property of the pressure distribution that can be gleaned from the right panels of Fig. 4 is that the maximum pressure first increases with increasing F, but eventually declines. While this transition happens very quickly in the case of small amplitude (panel (b)), it is more pronounced in the case of large amplitude (panel (f)). In fact, a similar behaviour can already be observed in the linear approximation. Close study of the formula (3.7) in [5] demonstrates that increasing the vorticity while keeping the amplitude constant results in overall higher pressure in the fluid.

Fig. 5 shows the results for the case when $\omega_0 < 0$. In this case, the results are more straightforward: the wavelength decreases with increasing F, the overall pressure is lower with increasing F, and the pressure profile is not monotone if F is sufficiently large.

The results shown in Figs. 4 and 5 agree qualitatively with the results obtained by Choi [21], where upstream propagating solitary waves get wider with increasing background vorticity, and downstream propagating solitary waves get narrower as the vorticity gains strength.

Another interesting aspect of surface waves with strong vorticity is shown in Fig. 6. The pressure contour lines depicted in this Figure suggest that the fluid pressure is actually below atmospheric pressure near the crest of the wave. While this

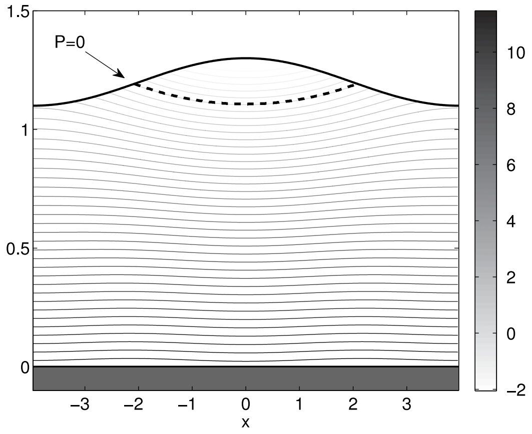

Fig. 6. Pressure contour lines for a periodic wave with $\alpha = 0.0886$ and $F = 1.2$. The non-dimensional pressure variation is from 11.72 to −2.07. The curve on which the pressure is equal to atmospheric is indicated as a dotted line, and marked $P = 0$.

behavior appears paradoxical at first glance, a heuristic physical explanation of the fact that the wave does not collapse is that the strong shear current forces the pressure to be negative at the tip of the wave [4]. It appears that a similar finding has also been presented in the work of Teles da Silva and Peregrine [4] on numerical integration of the steady Euler equations (2.3)–(2.5) and (2.8). However, in the context of simplified long-wave model equations both the pressure non-monotonicity depicted in Figs. 4 and 5 and the negative pressure shown near the wavecrest in Fig. 6 appear to be new results.

Acknowledgment

This research was supported in part by the Research Council of Norway.

References

[1] D.H. Peregrine, Interaction of water waves and currents, Adv. Appl. Mech. 16 (1976) 9–117.
[2] R.S. Johnson, A Modern Introduction to the Mathematical Theory of the Water Waves, Cambridge University Press, 1997.
[3] T.B. Benjamin, The solitary wave on a stream with an arbitrary distribution of vorticity, J. Fluid Mech. 12 (1962) 97–116.
[4] A.F. Teles da Silva, D.H. Peregrine, Steep, steady surface waves on water of finite depth with constant vorticity, J. Fluid Mech. 195 (1988) 281–302.
[5] M. Ehrnström, G. Villari, Linear water waves with vorticity: rotational features and particle paths, J. Differential Equations 244 (2008) 1888–1909.
[6] T.B. Benjamin, M.J. Lighthill, On cnoidal waves and bores, Proc. R. Soc. Lond. Ser. A 224 (1954) 448–460.
[7] A. Constantin, M. Ehrnström, E. Wahlén, Symmetry of steady periodic gravity water waves with vorticity, Duke Math. J. 140 (2007) 591–603.
[8] A. Constantin, J. Escher, Symmetry of steady periodic surface water waves with vorticity, J. Fluid Mech. 498 (2004) 171–181.
[9] A. Constantin, W. Strauss, Exact steady periodic water waves with vorticity, Comm. Pure Appl. Math. 57 (2004) 481–527.
[10] A. Constantin, E. Varvaruca, Steady periodic water waves with constant vorticity: regularity and local bifurcation, Arch. Ration. Mech. Anal. 199 (2011) 33–67.
[11] V.M. Hur, Exact solitary water waves with vorticity, Arch. Ration. Mech. Anal. 188 (2008) 213–244.
[12] H. Kalisch, A uniqueness result for periodic traveling waves in water of finite depth, Nonlinear Anal. 58 (2004) 779–785.
[13] E. Varvaruca, On some properties of traveling water waves with vorticity, SIAM J. Math. Anal. 39 (2008) 1686–1692.
[14] E. Wahlén, On steady gravity waves with vorticity, Int. Math. Res. Not. 2004 (54) (2004) 2881–2896.
[15] Y. Kang, J.M. Vanden-Broeck, Gravity-capillary waves in the presence of constant vorticity, Eur. J. Mech. B Fluids 19 (2000) 253–268.
[16] J. Ko, W. Strauss, Effect of vorticity on steady water waves, J. Fluid Mech. 608 (2008) 197–215.
[17] J. Ko, W. Strauss, Large-amplitude steady rotational water waves, Eur. J. Mech. B Fluids 27 (2008) 96–109.
[18] J.-M. Vanden-Broeck, Steep solitary waves in water of finite depth with constant vorticity, J. Fluid Mech. 274 (1994) 339–348.
[19] J.-M. Vanden-Broeck, Periodic waves with constant vorticity in water of infinite depth, IMA J. Appl. Math. 56 (1996) 207–217.
[20] W. Choi, Nonlinear evolution equations for two-dimensional surface waves in a fluid of finite depth, J. Fluid Mech. 295 (1995) 381–394.
[21] W. Choi, Strongly nonlinear long gravity waves in uniform shear flows, Phys. Rev. E 68 (2003) 026305.
[22] E. Wahlén, Hamiltonian long-wave approximations of water waves with constant vorticity, Phys. Lett. A 372 (2008) 2597–2602.
[23] A. Constantin, W. Strauss, Pressure beneath a Stokes wave, Comm. Pure Appl. Math. 63 (2010) 533–557.
[24] A. Ali, H. Kalisch, Mechanical balance laws for Boussinesq models of surface water waves, J. Nonlinear Sci. 22 (2012) 371–398.
[25] T. Colin, F. Dias, J.-M. Ghidaglia, On rotational effects in the modulations of weakly nonlinear water waves over finite depth, Eur. J. Mech. B Fluids 14 (1995) 775–793.
[26] P. Karageorgis, Dispersion relation for water waves with non-constant vorticity, Eur. J. Mech. B Fluids 34 (2012) 7–12.
[27] S.H. Doole, J. Norbury, The bifurcation of steady gravity water waves in (R, S) parameter space, J. Fluid Mech. 302 (1995) 287–305.
[28] V. Kozlov, N. Kuznetsov, The Benjamin–Lighthill conjecture for steady water waves (revisited), Arch. Ration. Mech. Anal. 201 (2011) 631–645.
[29] S.H. Doole, The pressure head and flowforce parameter space for waves with constant vorticity, Quart. J. Mech. Appl. Math. 51 (1998) 61–72.
[30] H. Kalisch, J. Lenells, Numerical study of traveling-wave solutions for the Camassa–Holm equation, Chaos Solitons Fractals 25 (2005) 287–298.
[31] J. Lenells, Traveling wave solutions of the Camassa–Holm equation, Licentiate Thesis, Lund University, 2004.